RESEARCH PAPER

Effect of ZrSiO$_4$/ZnO Ratio on the Properties of Opaque Glazes Used in -Ceramic Sanitary-Ware Industry

S. Benkacem[1]*, K. Boudeghdegh[1], F. Zehani[2] and Y. Belhocine[3]

* bekacemsamra@gmail.com

[1] Laboratory of Applied Energetics and Materials. University of Mohammed Seddik Ben Yahia- Jijel, Algeria.

[2] Laboratory of Materials Study. University of Mohammed Seddik Ben Yahia- Jijel, Algeria.

[3] Department of Petrochemical and Process Engineering, 20 August 1955 University of Skikda, Algeria.

Abstract: *This paper focuses on the effect of the ZrSiO$_4$/ZnO ratio on the properties of the glaze to be used on ceramic sanitary-ware. Structural and morphological characterization of these glazes was identified by XRD, SEM, FTIR, and Raman Spectroscopy. Furthermore, thermal properties of the glazes were determined by DTA and TG techniques. Besides, flexural strength, Vickers microhardness, whiteness, and chemical resistance of the glazes were investigated experimentally. XRD analysis showed that zircon and quartz the crystalline phases in the fired glaze layer. It was found that an increase of the ZrSiO$_4$/ZnO weight ratio from 3.85 to 67, causes an increase in the zircon crystallite particle size from 203.90 to 288.86 Å. From DTA, it was observed that by increasing ZrSiO$_4$/ZnO ratio, the crystallization temperature of zircon decreases. The glaze exhibits the highest whiteness value when the ratio of ZrSiO$_4$/ZnO became 12.60.*

Keywords: *Glaze, Ceramic sanitary-ware, ZrSiO4/ZnO ratio, Vickers Microhardness, Whiteness.*

1. INTRODUCTION

A ceramic raw glaze can be prepared from a mixture of specified raw materials such as alumina, kaolin, wollastonite, silica, feldspar, calcite, talc, dolomite, zinc oxide [1], stannic oxide, zirconia and zircon [2]; after being ground and applied onto a ceramic body. This mixture transforms either wholly or partially into a vitrified coat during a firing process [3]. Glazes are used to provide waterproofing protection to bodies, increase the mechanical durability, chemical inertness, abrasion and scratch resistance [4,5]. They are also appreciated for their aesthetic aspects [6]. (color, transparency, opacity, glossiness, smoothness, whiteness, etc.). In general, a highly opaque glaze is favorable for sanitary-ware products. The glaze opacity is obtained by the interaction between the crystalline phase that is dispersed in the glassy matrix and the incident light, resulting in the reflection and dispersion of the light. Thus, the greater the difference between the refractive indexes of the opacifier and the glassy matrix, the higher the opacity [7].

Zircon (ZrSiO$_4$) is often used in ceramic glazes as an opacifier, due to its high refractive index [8]. It is a highly refractory mineral [9], with a high melting point, low coefficient of thermal expansion, high thermal conductivity [10], high hardness and low solubility [11]. It is the most commonly used opacifier for ceramic glazes [12]. A major characteristic of zircon is the strength of the ZrO$_2$-SiO$_2$ bonds so that significant amounts of energy are needed to break these bonds [13]. Several studies have investigated the effect of added zircon on the properties of glazes. In this context, Castilone et al. [14]. addressed the crystallization of zircon in stoneware glazes as a function of its amount added to the glaze. The authors concluded that the quantity of zircon that crystallizes is a function of the amount of zircon added. When zircon additions are lower than 3 wt.%, most of it is dissolved into the melt and does not, afterward, recrystallize in the glaze. From 3 to 13 wt.%, more ZrSiO$_4$ crystallizes in proportion to the amount added. When the ZrSiO$_4$ addition is superior to13 wt.%, all the zircon is crystallized.

Usually, ZnO additions improve the glossiness of glaze and decrease the viscosity. This promotes the spreading of the melt over the substrate leading to the formation of a uniform layer. ZnO increases the surface tension of the glaze [15] and contributes to glaze opacity which leads to the formation of a high-quality glaze [16,17] The role of ZnO in glazes generally resembles that of alkaline earth oxides. Also, the dissolution rate of ZnO is somewhat faster at slightly lower temperatures than that of alkaline earth oxides. According to Tulyaganov et al., ZnO favors the early formation of the glassy matrix, resulting in highly homogeneous and dense structures [18]. The introduction of small amounts of ZnO (<2%) into glazes enhances the fusion and promotes a smooth perfect surface. When the amount of ZnO increases in the glaze, it acts as a refractory, and saturation of the glaze with ZnO results in crystalline texture [19]. Also, the opacity of a zircon bearing glaze will increase, in the presence of ZnO [20].

Because zircon and ZnO are among the most important oxides commonly used in the ceramic sanitary-ware, we have investigated in this work the impact of $ZrSiO_4/ZnO$ ratio on the physicochemical properties of sanitary-ware glazes. Moreover, this research aims to define the optimum glaze composition for obtaining better whiteness and higher mechanical properties.

2. EXPERIMENTAL PROCEDURE

2.1. Sample Preparation

In the present work, nine formulations of sanitary-ware glazes with varying $ZrSiO_4/ZnO$ ratio have been experimentally investigated. The starting raw materials used for the preparation of the glazes were kaolin Remblend denoted as RMB, sodium feldspar, quartz, calcium carbonate, dolomite, zircon, and ZnO; all are of industrial grade. More precisely, kaolin RMB was provided by Imerys Minerals Ltd; it originates from a large open pit in kaolinized granite near St. Austell, Cornwall, UK. Sodium feldspar was derived from Çine, Aydin of Turkey. Quartz, calcium carbonate, and dolomite were used respectively from different regions in Algeria, Bir el-Ater (Tebessa), Constantine, and Djelfa. Zircon was provided by Chilches Materials under the brand MICROZIR, Castellón, Spain. ZnO was supplied by Maghreb conception Industry (MCI) from Algeria. Chemical compositions were determined with the X-ray fluorescence spectrometer Rigaku ZSX Primus IV (see Table 1). The proportions of materials used in the glazes and the $ZrSiO_4/ZnO$ ratio are reported in Table 2 (in weight %).

To prepare the glazes, the raw materials, in suitable proportions were wet milled up to 1%

Table 1. Chemical compositions of raw materials (wt.%).

Oxides	Kaolin RMB	Hycast VC	Sodium feldspar	Quartz	Calcium carbonate	Dolomite	$ZrSiO_4$	ZnO
Al_2O_3	36.50	31	18	0.45	0.09	0.03	0	0
CaO	0.07	0.2	0.70	0.80	55.63	31.45	0	0
Fe_2O_3	1.01	1.2	0.06	0.40	0.02	0.03	0.08	0
MgO	0.30	0.4	0.20	0.13	0.01	20.38	0	0
K_2O	2	2.1	0.30	0.20	0	0	0	0
Na_2O	0.10	0.2	10	0.09	0	0	0	0
SiO_2	48	52	70	98.5	0.06	0.20	35	0
TiO_2	0.05	1	0.09	0.04	0	0.02	0.15	0
ZnO	0	0	0	0	0	0	0	98
ZrO_2	0	0	0	0	0	0	65	0
L. O. I *	12	12	0.40	0	43.80	47	1	1.90

*L. O. I = Loss. On. Ignition.

Table 2. Compositional range (wt.%) and ZrSiO$_4$/ZnO ratio of experimental raw glazes.

Glazes Notation	Kaolin RMB	Sodium feldspar	Quartz	Calcium carbonate	Dolomite	ZrSiO$_4$	ZnO	ZrSiO$_4$/ZnO ratio
G$_1$	6	34	26	10	7	13.50	3.50	3.85
G$_2$	6	34	26	10	7	14	3	4.66
G$_3$	6	34	26	10	7	15	2	7.50
G$_4$	6	34	26	10	7	15.50	1.50	10.33
G$_5$	6	34	26	10	7	15.75	1.25	12.60
G$_6$	6	34	26	10	7	16	1	16
G$_7$	6	34	26	10	7	16.25	0.75	21.66
G$_8$	6	34	26	10	7	16.50	0.50	33
G$_9$	6	34	26	10	7	16.75	0.25	67

residue using a sieve of 63 μm. This was followed by wet crushing of all raw materials in a porcelain jar for 3 h. The mixture: balls: water ratio was 1: 1: 0.5. To increase the milling efficiency [20], we used a deflocculating agent, namely, sodium silicate (Purity: 99.9%, grade ACS reagent, ratio SiO$_2$: NaO$_2$ superior to 2.4: 1). After this procedure, the obtained suspension particles were smaller than 63 μm. The fluidity of the glaze slurries was determined by a measurement of the time which the glaze slip passing through a 100 ml Ford cup (opening 2.6 mm); the Ford cup time values vary between 20 and 26 s. The density of the glaze suspension to cover the ceramics was 1.700-1.740 g/cm^3. This suspension was applied on dried ceramic bodies by spraying, using a compressed-air sprayer and then fired in a tunnel kiln for 21 h at a maximum temperature of 1250 °C under industrial conditions, i.e. oxidizing atmosphere. It should be noted that the ceramic bodies were provided by the Sanitary Ceramics Society (SCS) Company of El-Milia-Algeria, which contains 27 wt. % kaolin RMB, 27 wt.% ball clay (Hycast VC was provided by Imerys Minerals Ltd), 16 wt.% sodium feldspar and 30 wt. % quartz. The mean thickness of applied glazes was in the range of 0.2-0.4 mm after the firing cycle.

A computed Seger formula [21, 22] is given in Table 3. These values correspond to those found in the case of successful glazes in ceramic sanitary-ware, where SiO$_2$ is the major oxide for all samples ranging from 2.238 to 2.515, while Al$_2$O$_3$ content ranges from 0.199 to 0.220.

2.2. Methods of Characterization

The crystalline phases were identified by X-ray diffraction with Advance Bruker D8 diffractometer using Cukα radiation (λ=1.5406 Å). X-ray patterns were recorded in the 2θ range from 10 to 70°. Crystallite size D of the phase was estimated from X-ray using the Scherrer equation (1) [23]:

Table 3. Computed Seger formula of the studied glazes.

	Na$_2$O	K$_2$O	CaO	MgO	ZnO	Al$_2$O$_3$	Fe$_2$O$_3$	SiO$_2$	TiO$_2$	ZrO$_2$
G$_1$	0.129	0.007	0.601	0.164	0.100	0.199	0.002	2.238	0.002	0.165
G$_2$	0.131	0.006	0.609	0.166	0.087	0.202	0.002	2.277	0.002	0.174
G$_3$	0.135	0.006	0.628	0.171	0.060	0.208	0.002	2.359	0.002	0.192
G$_4$	0.137	0.007	0.637	0.174	0.045	0.211	0.002	2.402	0.002	0.201
G$_5$	0.138	0.007	0.642	0.175	0.038	0.213	0.002	2.424	0.002	0.206
G$_6$	0.139	0.007	0.647	0.176	0.031	0.215	0.002	2.446	0.002	0.211
G$_7$	0.140	0.007	0.652	0.179	0.023	0.216	0.002	2.469	0.002	0.216
G$_8$	0.141	0.007	0.657	0.179	0.016	0.218	0.002	2.492	0.002	0.221
G$_9$	0.142	0.007	0.662	0.180	0.008	0.220	0.002	2.215	0.002	0.226

$$D = \frac{K\lambda}{\beta \cos(\theta)} \qquad (1)$$

where D is the grain average size (Å), K is a constant (of the order of about 0.9, known as the Scherrer constant), λ is the X-ray wavelength, β is the full width at half maximum (FWHM) of the peak (radians) and θ is the Braggs angle (degree).

The morphology of crystalline particles and microstructure of the glazed layer were investigated using a Scanning Electron Microscope (SEM) (WD S, JEOL JSM 6360LV).

The infrared transmission spectra were obtained using the same weight of the glazes powder dispersed in KBr pellets (Purity: 99.9%, FTIR spectroscopic grade). The data is recorded by IR Affinity Shimadzu Japan spectrophotometer in the range 1400-400 cm^{-1}. Information on the chemical structure [24] of the studied glazes, was inspected also by Raman spectroscopy. Raman spectra were obtained using a Raman spectrometer LabRam HR (Horiba) in the range of 100 to 1200 cm^{-1}. The 632.8 nm line of an Nd: YAG laser was used as the exciting radiation with a power within 17 mW.

The thermal behavior of glazes was analyzed by differential thermal analysis and thermogravimetric (DTA/TG), carried out simultaneously on STA 409 equipment for temperatures up to 1200 ºC, with a heating rate of 10 ºC/min in air atmosphere. The mass of the sample used was 116 mg and alumina powder was used as reference material.

The percentage of water absorption (AA) was determined using the following procedure.The sample was dried for 12 h at 100 °C and its weight (mi) measured using a digital scale with 0.01 g accuracy; then, it was immersed in boiling water for 2 h, cooled for 12 h and its mass weighed (mf) again. The percentage of water absorption (AA) was calculated from the equation (2):

$$AA\% = 100\left(\frac{m_f - m_i}{m_i}\right) \qquad (2)$$

where m_f is the wet mass (g) and m_i is the dry mass (g).

This parameter is commonly used in the industry to quantify the degree of porosity and to estimate whether the prepared sanitary-ware glazes meet the technical requirements [25].

The flexural strength (S_{fl}) of the glazed specimen was measured after firing on a three-point bending test conducted on a NETSZH universal testing machine. The data is then converted to flexural strength by applying the formula (3):

$$S_{fl} = \frac{3}{2}\frac{PL}{bh^2} \qquad (3)$$

where P is the failure load (N), L is the distance between supports (90 mm), b is sample width (20 mm) and h is sample thickness (20 mm).

An Affri DM2D Digital Micro Hardness Tester with a Vickers diamond indenter was used to measure the microhardness of glazes surface, loading at 1000 gf, with an application time of 25 s. All indentations were performed on polished surfaces and cross-sections of the glazed layer. Fifteen measurements were made on different regions of each sample under laboratory conditions. The Vickers microhardness is calculated using the equation (4):

$$HV = 1.8544\frac{F}{d^2} \qquad (4)$$

where F is the applied test load in (N), d is the average of two indentation diagonal lengths in (μm) and 1.8544 is a geometrical constant of the diamond pyramid [26].

The whiteness was evaluated with a colorimeter Dr Langer micro color DATA STATION (according to DIN 5033 standard). The appearance of the surface of the glazes was also visually inspected in terms of homogeneity and the presence of defects (bubbles, cracks).

Chemical resistance of glazes is often classified visually after exposure to different aqueous solutions according to standard methods. In this work, the chemical resistance of all samples was tested according to the NF D14-506 and NF D14-508 standard tests, by soaking test pieces in size 24 mm × 24 mm at room temperature in test solutions like hydrogen peroxide 20 volumes (6% W/V, grade ACS reagent), potassium permanganate (0.6 M, purity: 98.3%, grade ACS reagent) [27] and citric acid (10%, purity: 99.5%, grade ACS reagent). Afterward, they were treated with dilute hydrochloric acid (3%, grade ACS reagent) and an aqueous solution of sodium hydroxide as

alkali (3%, purity: 99%, grade ACS reagent) for 7 days at 20 °C [28]. The glazes were then visually inspected to verify possible changes in color and surface morphology.

Based on the dependence of the properties of glazes upon composition, it is possible to compute the coefficients of thermal expansion. The thermal expansion coefficient (, which influences the adherence of the glaze onto the ceramic body, was calculated according to the Appen formula (5). This law states that each oxide has a different contribution to the final α value [29]:

$$\alpha = \frac{10^{-7}}{100} \sum \alpha_i \, p_i \qquad (5)$$

where is the oxide factors (Appen series) (°C^{-1}) and is the molar percentage of each oxide present in the glaze.

3. RESULTS AND DISCUSSIONS

3.1. X-ray Diffraction Analysis

Fig. 1 shows the X-ray diffraction pattern of the fired samples G$_1$ and G$_9$. The diffraction peaks could be attributed to zircon, as identified by using the JCPDS database file 06-0266 and quartz JCPDS database file 01-0649. It may be observed that zircon is the main crystalline phase for different ratios of ZrSiO$_4$/ZnO. It is clear that zircon remains stable even after a firing 1250 °C [30].
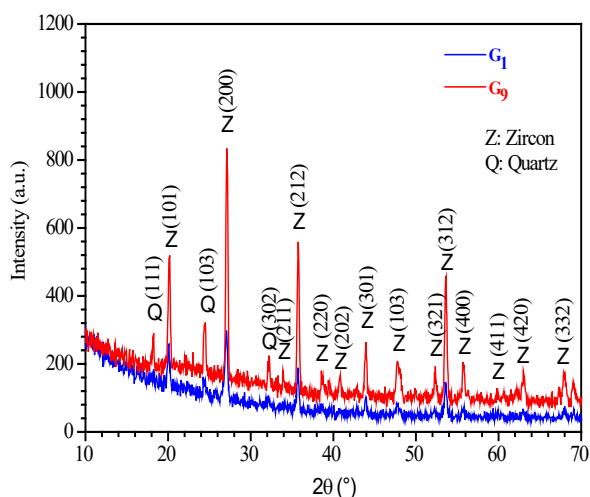

**Fig. 1.** X-ray diffraction patterns of G1 and G9 glazes after firing at temperature 1250 °C.

The values of crystallite grain sizes deduced from the most intense line broadening of the (200) zircon peak (2θ=27.11°) which estimated from the Scherrer equation for samples G$_1$ and G$_9$ are 203.90 and 288.86 Å, respectively. Noteworthy, the crystallite size increases with the increasing ZrSiO$_4$/ZnO ratio. ZnO promotes zircon crystallization during the heating process and leads to very stable opaque coatings [31]. Voevodin reported that the optimum size of the grains of the opacifier that provided maximum dulling is 0.2-1.0 µm [32]. Besides, the existence of zircon crystals with particle size approaching the wavelength of incoming light improves light to scatter and thus, ensures opacification 13.

3.2. Scanning Electron Microscopy (SEM)

The microstructural observations of glazes G$_1$, G$_4$, G$_5$ and G$_9$ with different ZrSiO$_4$/ZnO ratios are shown in Fig. 2. As can be seen all of them exhibit similar features. The surface of all glazes is completely densified and some white zircon crystals (indicated by rectangles in Fig. 2) are observed. Also, pieces of the dark zone (indicated by circles in Fig. 2) which are surrounded by clusters of zircon crystals can be found. These dark areas seem to be the quartz crystals, according to the X-ray diffraction pattern shown in Fig. 1. Also, the zircons and quartz crystals are dispersed in the glass matrix (indicated by arrows in Fig. 2). Schabbach et al. studied the effect of grain and shape of zircon crystals on the opacity of ceramic glaze. They found that fine particles are always needed for high opacity [33]. Wang et al. studied the clustering of zircon in raw glaze and found that the cluster of zircon crystals are the results of the combined effects of the releasing of gas and liquid phase formed from the melting of fusible components. In step of formation of the liquid phase, bubbles enable zircon to move and aggregate at their boundaries. As the gas releasing, these crystals are difficult to return to their initial position because of the high viscosity of the melt [34].

3.3. FTIR and Raman Spectroscopy

In Fig. 3, the FTIR spectra of the studied glazes are presented. It shows broad bands due to the overlapping effects of vibration and rota-

| Fig. 2-a | Fig. 2-b | Fig. 2-c | Fig. 2-d |
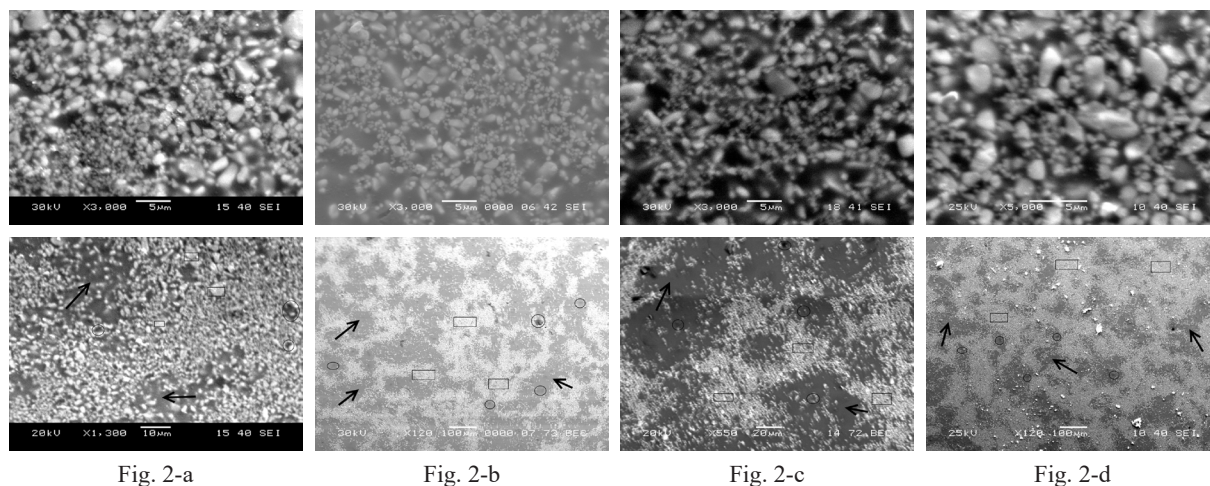
Fig. 2. SEM micrograph of the a) G1 sample, b) G4 sample, c) G5 sample and d) G9 sample, showing zircon (indicated by rectangles), quartz (indicated by circles) and glass phase (indicated by arrows).
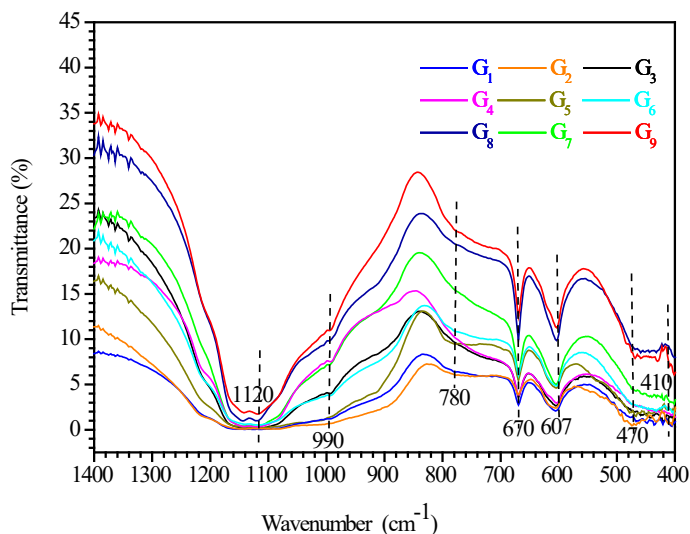
Fig. 3. FTIR spectra of the elaborated glazes.

tion of structural groups which are characteristic of solids in the vitreous state. We note the presence of at least three bands at 1140, 780, and 470 cm^{-1} [35,36]. It can be observed that all the bands are quite broad. From this observation, we concluded that the studied glazes have a disordered structure. The characteristic IR band of pure silica corresponding to the asymmetric vibration of the bridging Si–O–Si bands within SiO_4 tetrahedra is observed at 1140 cm^{-1} [36]. This band is moved to a lower frequency at 1120 cm^{-1} in G_8 and G_9 indicating that Si–O–Si is perturbed by the presence of a significant amount of zircon [37]. Moreover, the band at 780 cm^{-1}, is related to Si–O–(Si, Al) symmetric stretching vibrations between SiO_4

units. The band appears near 607 cm^{-1} and thus could be ascribed to the Si–O–Zr vibration modes [38]. It is noteworthy that the transmittance of this band increases with the increase in the amount of the introduced zircon. Furthermore, the bands at 470 and 410 cm^{-1}, are due to the bending vibration of O–Si–O and O–Al–O [39].

The Raman spectra of the two glazes G_1 and G_9 are represented in Fig. 4. While the strong band anti-symmetric stretching of the SiO_4 group is observed near 1008 cm^{-1}, the band near 975 cm^{-1} is assigned as a Si-O stretching band [40]. Other Raman bands of $ZrSiO_4$ at 438, 357, and 224 cm^{-1} are present in the spectra of the two glazes [41]. Intense external lattice vibrations occurring in the
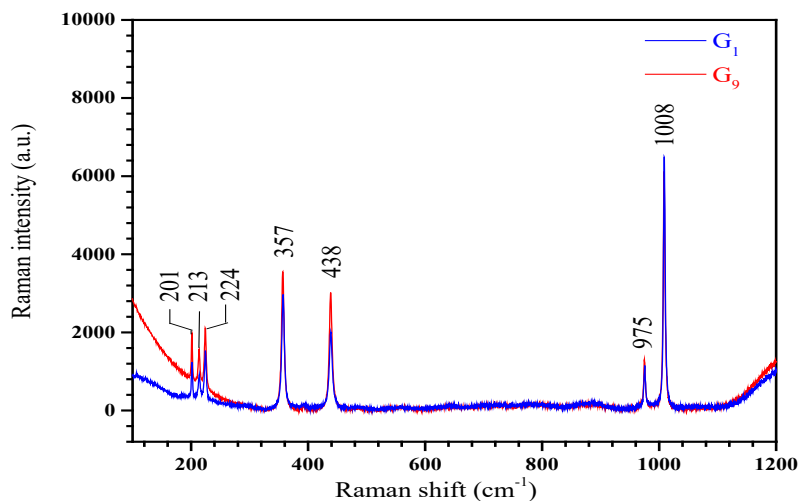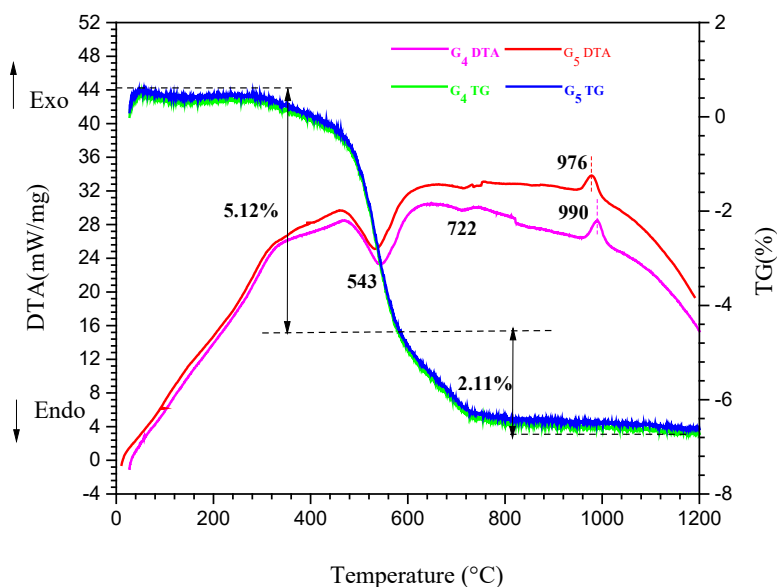
Fig. 4. Raman spectra of the two glazes G1 and G9.

Fig. 5. DTA/TG analysis of the glazes G_4 and G_5 samples.

bands 224, 213, and 201 cm⁻¹, in the G_1 and G_9 spectra, confirm the presence of the zircon crystalline phase with a tetragonal unit cell 42..

3.4. Thermal Analysis

Fig. 5 shows DTA/TG graphs of the G_4 and G_5 samples. In the temperature range 200-600 °C, there is a change in mass revealed by the TG curve; it is due to the removal of water adsorbed into the pores and dehydroxylation of the kaolinite [43]. The loss of mass calculated from the TG curve ranges from 5.02 to 5.12% in G_4 and G_5. The endothermic effect in the range 542-580 °C, was

observed in DTA associated with the dehydroxylation of kaolinite [44]. Small endothermic peaks at about 710 and 825 °C are related to the decomposition of calcium carbonate and dolomite, respectively [45,46], with a loss of mass equivalent to 2.11%. It is worth noting that the exothermic peak associated with zircon crystallization generally occurs at about 990 °C [47,48]. Thus, from DTA thermographs, it is evident that the exothermic peak position moves to higher temperatures with the decrease of theZrSiO$_4$/ZnO ratio. The temperature of the crystallization of zircon in the sample G_4 is estimated 990 °C, which is higher than that of sample G_5 with ZrSiO$_4$/ZnO equal to
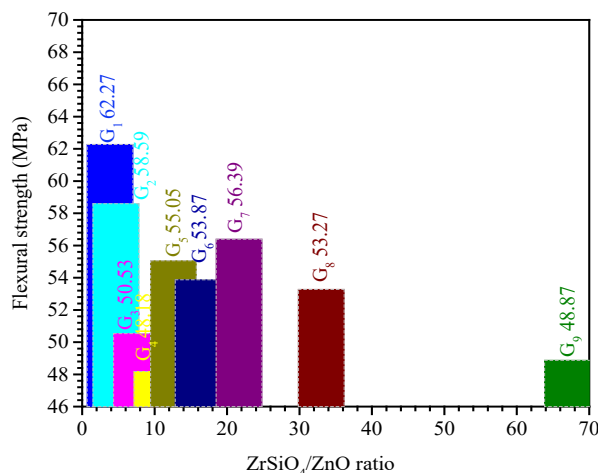
Fig. 6. Effect of $ZrSiO_4/ZnO$ ratio on flexural strength of glazes.

12.60 estimated at 976 °C; therefore, the crystallization temperature of glaze appears to scale with the decrease of $ZrSiO_4/ZnO$ ratio.

3. 5. Percentage of Water Absorption, Flexural Strength, Vickers Microhardness and Whiteness of Experimental Glazes

Results of the percentage of water absorption study of the glazes are presented in Table 4; it can be seen that the percentage of water absorption values range from (0.05 ± 0.02) to $(0.15 \pm 0.05\%)$. The reason for these low values could be a high degree of vitrification [49]. This aspect is linked to the formation of the liquid phase at high firing temperature which penetrates the pores, closing them and isolating adjacent pores, promoting thus the densification between particles and reducing porosity [50].

Fig. 6 shows the influence of the $ZrSiO_4/ZnO$ ratio on the flexural strength of glazed-ceramic specimens, as a function of the $ZrSiO_4/ZnO$ ratio. As mentioned above, all the glazes with different compositions featured good densification degrees, with main crystals phases as zircon and quartz dispersed in the glass phase with low porosity. This is ascribed to the high values of flexural strength (see Table 4). The flexural strength of glazed sample G1 with 3.85 $ZrSiO_4/ZnO$ ratio is at its maximum, which is $(62.27 \pm 4.72$ MPa). It is interesting to note, that the flexural strength of all samples ranges from $(48.18 \pm 2.04$ MPa) to $(62.27 \pm 4.72$ MPa). These values are satisfactory in terms of flexural strength for glazed sanitary-ware.

Microhardness results are presented in Table 4. It should be pointed out that the increase of porosity in the glaze surfaces would result in

Table 4. Percentage of water absorption, flexural strength, microhardness of Vickers and whiteness of the prepared glazes.

Glazes	Percentage of water absorption (%)	Flexural strength (MPa)	Microhardness (MPa)	Whiteness (%)
G_1	0.05 ± 0.02	62.27 ± 4.72	4858.41 ± 470	75.20
G_2	0.06 ± 0.03	58.59 ± 5.34	5877.05 ± 129	79.70
G_3	0.14 ± 0.02	50.53 ± 2.21	6026.97 ± 304	79.50
G_4	0.06 ± 0.03	48.18 ± 2.04	6486.40 ± 214	82.20
G_5	0.11 ± 0.06	55.05 ± 6.67	6165.35 ± 271	87.00
G_6	0.15 ± 0.05	53.87 ± 4.03	6023.91 ± 820	79.50
G_7	0.11 ± 0.04	56.39 ± 3.45	5875.82 ± 201	84.40
G_8	0.11 ± 0.01	53.27 ± 2.10	6587.81 ± 241	82.40
G_9	0.06 ± 0.02	48.87 ± 3.98	5729.35 ± 223	85.80

the occasional formation of irregular indentation impressions. As mentioned above, the porosity values, measured through the percentage of water absorption (%), are very low that leads to the improvement of surface quality of samples. More importantly, the microhardness of glazes is not only related to both crystalline and glassy matrixes [51], but also to the porosity of the glaze surface [52]. The decreasing of porosity values and enrichment of the glass phase with zircon crystals contribute to improving the microhardness. The microhardness of the crystal is greater than that of the glass. The highest value (6587.81 ± 241 MPa) was registered on sample G_8, with a $ZrSiO_4$/ZnO ratio of 33; which is due to the presence of a large number of zircon crystals in the glassy matrix.

According to Table 4, the values of whiteness are close to 100%; typical of whiteness for ceramic sanitary-ware. An increase in the whiteness value (87.00%) is observed for G_5 glaze, due to the presence of zircon crystals. To understand this, Aparici et al. [53] examined the effect of the firing cycle on the whiteness of a glaze. The authors found a direct proportionality between the volume fraction of zircon crystals and the whiteness index of the glaze. However, decreasing ZnO content in glaze reduces the whiteness; because ZnO is linked to the improvement of color development and augments the brightness as well as it enhances the glaze surface quality [47]. These desirable effects of ZnO in opaque glazes, appear in connection with the presence of zircon. The surface appearance of all glazes was homogeneous and defects- free (bubbles, cracks), because of the small amount of ZnO. It is known that large amounts of this oxide may cause crawling, pin holing and pitting [54].

The highest value for the whiteness (87.00%) together with a high value for flexural strength (55.05 ± 6.67 MPa) and high microhardness of Vickers (6165.35 ± 271 MPa) were measured for the sample G_5, with a $ZrSiO_4$/ZnO ratio of 12.60.

3.6. Chemical Resistance of the Obtained Glazes

Based on NF D14-506 and NF D14-508 standards, all glazes are classified as Class AA; there are no significant changes on the surfaces of the samples after the tests. All glazes have shown very good chemical resistance to both dilute hydrochloric acid and a solution of sodium hydroxide. This good resistance can be attributed to the presence of zircon which is thought to improve chemical resistance [55]. Moreover, the dissolution of zinc oxide into the glass phase increases significantly the chemical resistance of the resulting glaze 17, [56].

3.7. Theoretical Calculations

The thermal expansion coefficient is calculated and listed in Table 5. As the $ZrSiO_4$/ZnO ratio grows to 67, the thermal expansion coefficient decreased, and the glazed specimens become more thermally stable. This is due to a smaller thermal expansion coefficient mismatches between the glazes and the ceramic body, which is equal to 42.10×10^{-7} °C^{-1}. The thermal expansion coefficient of glazes should be 10% lower than the thermal expansion coefficient of the ceramic body 45., to ensure strong bonding in the glaze-ceramic system [57]. This is achieved by raising the zircon content as mentioned above. Consequently, this finding confirms the absence of crazing and cracking problem caused by strain effect due to the thermal expansion coefficient mismatch of the glaze and the body. Plesingerova et al. found that if the thermal expansion coefficient of the glaze be higher than that of the body, a considerable tensile stress which exceed the strength of glaze will crack it during cooling process. Also, the thinner layer of glaze (200-250 µm),

Table 5. Thermal expansion coefficient of the glazes.

Glazes	Thermal expansion coefficient ($\times 10^{-7}$ °C^{-1})
G_1	59.91
G_2	59.71
G_3	59.30
G_4	59.09
G_5	58.99
G_6	58.88
G_7	58.78
G_8	58.68
G_9	58.57

the richer the crack [58]. Besides the composition and phases of glazes, the flexural strength of glazed specimen depends on the difference in glaze-body thermal expansion coefficient mismatch and the thickness of interface layer between them. It seems that ZnO plays also role in decreasing the thermal expansion coefficient of the glaze [59].

4. CONCLUSIONS

We have evaluated the effect of $ZrSiO_4$/ZnO ratio on the properties of opaque glaze, and more importantly, we have determined the optimal composition. According to the results mentioned above, it can be said that:

1. XRD results identified zircon and quartz as a crystalline phases in glaze independently of the $ZrSiO_4$/ZnO ratio.
2. According to SEM, crystals of zircon and quartz embedded in the glassy matrix for different $ZrSiO_4$/ZnO ratios.
3. DTA/TG analysis suggested that the zircon crystallization temperature slightly increases with the decrease in $ZrSiO_4$/ZnO ratio.
4. The flexural strength of glazed ceramics not only depends on the composition and phases, but also on the difference in the glaze-body thermal expansion coefficient mismatch and the thickness of interface layer between them.
5. The optimal sample G5 corresponding to the $ZrSiO_4$/ZnO ratio of 12.60 has a high flexural strength (55.05 ± 6.67 MPa), high microhardness of Vickers (6165.35 ± 271 MPa) and in particular higher whiteness (up to 87%).
6. The results were satisfactory in terms of whiteness, surface texture and microhardness, and therefore, meet the requirements of standard tests for glazed ceramic sanitary-ware.

REFERENCES

1. Turner, A., "A ceramic monthly handbook, Glazes: Materials, Recipes and Techniques. Amer. Ceram. Soc. 600N". Cleveland AVe., Suite 210 Westerville, Ohio 43082 USA, 2004, 6.
2. Ryan, W., Properties of Ceramic Raw materials, 2nd Eds, Elsevier, 2013, 105.
3. Partyka, J. and Lis, J., "Chemical corrosion of sanitary glazes of variable grain size composition in acid and basic aqueous solution media". Ceram. Int., 2012, 38, 1, 553-560.
4. Gorodylova, N., Dohnalova, Z., Kostal, P., Sulcova, P. and Vlcek, M., "Impact of particle size reduction on glaze-melting behaviour Description by heating microscopy and Vogel-Fulcher-Tamman equation". J. Therm. Anal. Calorim., 2014, 116, 2, 605-612.
5. Singer, F. and Singer, S. S., Industrial Ceramics, London, Chapman. Hall, 1963, 525.
6. Kavanova, M., Klouzkova, A. and Klouzek, J., "Characterization of the interaction between glazes and ceramic bodies". J., Ceram. Silik., 2017. 61, 3, 267-275.
7. Israil, L. I., Koseoglu, K. and Cengizler, H., "Effect of silver oxide on colour variation and gloss of an opaque glaze". J. Trans. Ind. Ceram. Soc., 2014, 73, 1, 22-30.
8. Shabbat, M., Bondioli, F. and Fredel, M. C., "Colouring of opaque ceramic glaze with zircon pigments: Formulation with simplified Kubelka–Munk model". J. Eur. Ceram. Soc., 2011, 31, 5, 659-664.
9. Kaiser, A., Lobert, M. and Telle, R., "Thermal stability of zircon (ZrSiO4)". J. Eur. Ceram. Soc., 2008, 28, 2199-2211.
10. Brown, J. R., Foseco Ferrous Foman's Handbook, 11th Ed, Chapter 12, Sands and green sand, Butterworth-Heinemann, 2000, 151.
11. Sarjahani. R, Sheikhattar, M., Javadpour. S and Hashemi. B., "The effect of opacifiers on surface roughness of ceramic glazes". Iran. J. Mat. Sci. Eng., 2016, 13,1, 37-42.
12. Atkinson, I., Smith, M. E. and Zaharescu, M., "Examining correlations between composition, structure and properties in zircon-containing raw glazes". Ceram. Int., 2012, 38, 3, 1827-1833.
13. Snyders, E., Potgieter, J. H. and Nel, J. T., "The upgrading of an inferior grade zircon to superior opacifier for sanitary ware and glazes". J. S. Afr. Inst. Min. Metall., 2005, 105, 7, 459-464.
14. Castilone, R.J., Sriram, D., Carty, W. M. and Snyder, R. L., "Crystallization of Zircon in

Stoneware Glazes". J. Am. Ceram. Soc., 1999, 82, 10, 2819-2824.

15. Hamer, F. and Hamer. J., The potter's dictionary of materials and technique, 5 ed, University of Pennsylvania press, 2004, 93.

16. Jamaludin, A. R., Kasim, S. R. and Ahmad, Z. A., "The effect of CaCo3 addition on the crystallization behavior of ZnO crystal glaze fired at different gloss firing and crystallization temperatures". Sci. Sinter., 42, 3, 2010, 345-355.

17. Casasola, R., Rincon, J. Ma. and Romero, M., "Glass-ceramic glazes for ceramic tiles - a review". J. Mater. Sci., 47, 2, 2012, 553-582.

18. Tulyaganov, D. U., Agathopoulos, S., Fernandes, H. R. and Ferreira, J. M. F., "The influence of incorporation of ZnO-containing glazes on the properties of hard porcelains". J. Eur. Ceram. Soc., 2007, 27, 2, 1665-1670.

19. Pekkan, K., "The thermal and microstructural behavior of a R2O-RO-(ZnO)-Al_2O_3-(TiO_2)-SiO_2 based macro-crystalline raw glaze system". Ceram. Int., 2015, 41,6, 7881-7889.

20. Romero, M., Rincon, J. Ma. and Acosta, A., "Crystallisation of a zirconium-based glaze for ceramic tile coatings". J. Eur. Ceram. Soc., 2003, 23, 10, 1629-1635.

21. Wood, N., "Chinese Glazes: Their Origins, Chemistry, and Recreation, University of Pennsylvania Press", 1999, 257.

22. Norsker, H. and Danisch, J., "Glazes- for the Self - Reliant Potter, Springer, Fachmedien, Wiesbaden", 1993, 119.

23. Paradeep, T., "A textbook of Nanoscience and Nanotechnology", New delhi, New York, 2012, 127.

24. Smith, E. and G. Dent, "Modern Raman Spectroscopy A Practical Approach, John Wiley & Sons", Ltd, The Atrium, Southern Gate, Chichester, West Sussex PO19 8SQ, England, 2005, 1.

25. Bernasconi, A., Diella, V., Pagani, A., Pavese, A., Francescon, F., Young, K., Stuart, J. and Tunnicliffe, L., "The role of firing temperature, firing time and quartz grain size on phase-formation, thermal dilatation and water absorption in sanitary-ware vitreous bodies". J. Eur. Ceram. Soc., 2011, 31, 8, 1353-1360.

26. Guder, H. S., Sahin, E., Sahin, O., Gocmez, H., Duran, C. and Cetinkara, H. A., "Vickers and Knoop Indentation Microhardness Study of β-SiAlON Ceramic". Acta Phys. Pol., A. 2011, 120, 6, 1026-1033.

27. Venkatesh, G., Thenmuhil, D., Vidyavathy, S. M. and Vinothan, R., "Effect of addition of nano zirconia in ceramic glazes". J. Adv. Mat. Res.,

2014, 984-985, 488-494.

28. Yalcin, N. and Sevinc, V., "Utilization of bauxite waste in ceramic glazes". J. Ceram. Int., 2000, 26, 5, 485-493.

29. Amoros, J. L., Blasco, A., Carceller, J. V. and Sanz, V., "Acordo Esmalte-Suporte (II) Expansao Térmica de Suportes e Esmaltes Cerâmicos". Ceram. Ind., 1997, 2, 1/2, 8-16.

30. Eftekhari Yekta, B., Alizadeh, P. and Rezazadeh, L., "Synthesis of glass-ceramic glazes in the ZnO-Al2O3-SiO_2-ZrO2 system". J. Eur. Ceram. Soc., 2007, 27, 2311-2315.

31. Wang, S., Peng, C., Ming, L. and Jianqing, W., "Effect of ZnO on crystallization of zircon from zirconium- based glaze". J. Am. Ceram. Soc., 2013, 96, 7, 1-4.

32. Voevodin, V. I., "Unfritted opaque glaze for ceramic sanitarware". Steklo Keram., 2000, 7, 23-24.

33. Schabbach, L. M., Bondioli, F., Ferrari, A. M., Manfredini, T., Petter, C. O. and Fredel, M. C., "Influence of firing temperature on the color developed by a (Zr, V) SiO_4 pigmented opaque ceramic glaze". J. Eur. Ceram. Soc., 2007, 27, 1, 179-184.

34. Wang, S., CHeng, P., Zhilong, H., Jum, Z., Ming, L. and Jianqiny, W., "Clustering of zircon in raw glaze and its influence on optical properties of opaque glaze". J. Eur. Ceram. Soc., 2014, 34, 541-547.

35. Roy, B. N., "Infrared spectroscopy of lead and alkaline-earth aluminosilicate glasses". J. Am. Ceram. Soc., 1990, 73, 4, 846-855.

36. Atkinson, I., Teoreanu, I., Mocioiu, O. C., Smith, M. E. and Zaharescu, M., "Structure property relations in multicomponent oxide systems with additions of TiO2 and ZrO2 for glaze applications". J. Non-Cryst. Sol., 2010, 356, 44, 2437-2443.

37. Chandradass, J., Han, K. S and Bae, D. S., "Synthesis and characterization of zirconia- and silica-doped zirconia nanopowders by oxalate processing". J. Mater. Process. Technol., 2008, 206, 1-3, 315-321.

38. Popa, M., Kakihana, M., Yoshimura, M. and Calderon-Moreno, J. M., "Zircon formation from amorphous powder and melt in the silica-rich region of the alumina–silica–zirconia system". J. Non-Cryst. Sol., 2006, 352, 52-54, 5663-5669.

39. Lesniak, M., Partyka, J., Gajek, M. and Sitarz, M., "FTIR and MAS NMR study of the zinc aluminosilicate ceramic glazes". J. Mol. Struct., 2018, 1171, 17-24.

40. Gucsik, A., Zhang, M., Koeberl, C., Salje, E. K.

H., Redfern, S. A. T. and Pruneda, J. M., "Infrared and Raman spectra of ZrSiO4 experimentally shocked at high pressures". Mineral Mag., 2004, 68, 5, 801-811.

41. Atkinson, I., Angheln, E. M., Munteanu, C., Voicescu, M. and Zaharescu, M., "ZrO2 influence on structure and properties of some alkali lime zinc aluminosilicate glass ceramics". Ceram. Int., 2014, 40, 5, 7337-7344.

42. Nasdala, L., Irmer, G. and Wolf, D., "The degree of metamictization in Zircon: A Raman spectroscopic study". Eur. J. Mineral., 1995, 7, 3, 471-478.

43. Gasparini, E., Tarantino, S. C., Ghigna, P., Riccardi, M. P., Cedillo-González, E. I., Siligardi, C. and Zema, M., "Thermal dehydroxylation of kaolinite under isothermal conditions". Appl. Clay Sci., 2013, 80–81, 417-425.

44. Yeskis, D., Groos, A. F. K. V. and Guggenheim, S., "The dehydroxylation of kaolinite". Am. Mineral., 1985, 70, 159-164.

45. Levitskii, I. A. and Mazura, N. V., "Opacified glazes produced by high-temperature firing for sanitary ceramicware". Steklo Keram., 2005, 7, 21-24.

46. Wiedemann, H. G. and Bayer, G., "Note on the thermal decomposition of dolomite". Thermochim. Acta., 1987, 121, 479-485.

47. Pekkan, K. and Karasu, B., "Production of opaque frits with low ZrO2 and ZnO contents and their industrial uses for fast single-fired wall tile glazes". J. Mater. Sci., 2009, 44, 10, 2533-2540.

48. Pekkan, K. and Karasu, B., "Evaluation of borax solid wastes in production of frits suitable for fast single-fired wall tile opaque glass-ceramic glazes". Bull. Mater. Sci., 2010, 33, 2, 135-144.

49. Martini, E., Fortuna, D., Fortuna, A., Rubino, G. and Tagliaferri, V., "Sanitser, an innovative sanitary ware body, formulated with waste glass and recycled materials". Cerâmica., 2017, 63, 542-548.

50. Chen, Y., Zhang, Y., Chen, T., Liu, T. and Huang, J., "Preparation and characterization of red porcelain tiles with hematite tailings". Constr. Build. Mater., 2013, 38, 1083-1088.

51. Cai, J., Lv, M., Guan, K., Li, W., He, F., Chen, P., Peng, C., Rao, P. and Wu, J., "Effect of ZnO/MgO ratio on the crystallization and optical properties of spinel opaque glazes". J. Am. Ceram. Soc., 2017, 101, 4, 1754-1764.

52. Eftekhari Yekta, B., Alizadeh, P. and Rezazadeh, L., "Floor tile glass-ceramic glaze for improvement of glaze surface properties". J. Eur. Ceram.

Soc., 2006, 26, 16, 3809-3812.

53. Aparici, J., Moreno, A., Escardino, A., Amorós, J. L. and Mestre, S., "Estudio de la opacification en vidriados ceramicos de circonio utilizados en la fabrication de baldosas de revestimiento por monococcion". Proceedings of II World Congress on Ceramic Tile Quality, Castellon, Spain, 1994, 35-46.

54. O'Conor, E. F., Gill, L. D. and Eppler, R. A., "Recent developments in leadless glazes. Materials and Equipment–Whitewares" 86th annual Meeting, and the 1984 Fall Metting of the Materials, and Equipment Whitewares Divisions, 5, 11-12, 1984, 924-932.

55. Ezz-Eidin, F. M. and Nageeb, W. M., "Chemical resistance of some irradiated ceramic - glazes". Indian J. Pure Appl. Phys., 2001, 39, 8, 514-524.

56. Kim, S. K., Lee, S. M., Choi, E. S. and Kim, H. T., "Effect of zinc oxide addition on crystallization behavior and mechanical properties of a porcelain body". Whitewares and Materials: 105th annual Meeting of the American Ceramic society and the Whitewares and Materials Division fall Meeting, 2004, 25, 2, 3-14.

57. Levitskii, I. A., Barantseva, S. E. and Mazura, N. V., "Particulars of structure and phase formation in zirconium-containing frits and glazes". Steklo keram., 2009, 7, 25-28.

58. Plesingerova, B. and Kovalcikova, M., "Influence of the thermal expansion mismatch between body and glaze on the crack density of glazed ceramics". Ceram. Silik., 2003, 47, 3, 100-107.

59. M. Schwartz, "Encyclopedia of Materials, Parts and Finishes", 2. Ed., Boca. Raton. London. New York. Washington, 2002, 896.